Food Research 9 (3) : 67 - 75 (June 2025)
Journal homepage: https://www.myfoodresearch.com

FOOD RESEARCH

RESEARCH PAPER

Dynamic modelling of oil and water molecules of methylcellulose-coated fried potato during and in the post-frying condition

[1]Lee, X.F., [1,2,*]Naim, M.N., [3]Azmi, N.S.M., [1]Mohammed, M.A.P., [1,2]Othman, S.H., [3]Abu Bakar, N.F. and [4]Adam, F.

[1]*Department of Process and Food Engineering, Faculty of Engineering, 43400, Universiti Putra Malaysia, Serdang, Selangor, Malaysia*
[2]*Nanomaterials Processing and Technology Laboratory, Institute of Nanoscience and Nanotechnology, 43400, Universiti Putra Malaysia, Serdang, Selangor, Malaysia*
[3]*School of Chemical Engineering, College of Engineering, 40450, Universiti Teknologi MARA, Shah Alam, Malaysia*
[4]*Faculty of Chemical and Process Engineering Technology, 26300, Universiti Malaysia Pahang, Pahang, Malaysia*

Article history:
Received: 12 July 2024
Received in revised form: 13 September 2024
Accepted: 15 February 2025
Available Online: 21 May 2025

Keywords:
B-type starch,
Diffusion coefficient,
Dynamic simulation,
Methylcellulose,
Potato starch

DOI:
https://doi.org/10.26656/fr.2017.9(3).164

Abstract

This work investigated the migration of the oil and water molecules in methylcellulose (MC)-coated and uncoated potatoes during and after the deep-frying process. The research aimed to understand how the MC layer prevented the oil uptake due to water migration from the substrate to cooking oil along the frying process using molecular dynamic modelling techniques and validated by the experimental work. During the frying process, the diffusion coefficient from the mean square displacement (MSD) value of water in the frying oil, D_w, at the interfacial of MC-coated showed a greater value compared to the uncoated ones with a diffusion coefficient of 1.08 and 0.63 (10^{-4} cm^2/s), respectively. In the post-frying process, the D_w in the cooling frying oil was 0.94 and 0.08 ($10^{-4}cm^2/s$), respectively. Both coated and uncoated layers provide intense water flux against the oil penetration along the process. A consistently low diffusion coefficient of oil into starch, D_o of 0.14 and 0.13 (10^{-4} cm^2/s), was noticed during and in the post-frying process. Meanwhile, lower diffusion coefficient D_w values in uncoated samples were not caused by oil penetration but due to the large amounts of trapped surface oil known as structural oil in the crust layer. The evidence was shown by low D_o in the uncoated potato's region with a diffusion coefficient during and after the frying process of 0.35 and 0.07 (10^{-4} cm^2/s), respectively. The phenomenon was proven in the experimental work whereby more significant pore areas were noticed in uncoated ones compared with the MC-coating substrate of 25107 vs 24000 mm^2, respectively, at various MC concentrations. Both the model and the experimental results agree on the significant trend of oil uptake reduction, as the MC layer promotes sufficient water flux out from the fried substrate to prevent oil penetration into the starch along the frying process.

1. Introduction

The phenomenon of water diffusivity and oil uptake in the post-frying process is complicated to predict when imbibition of surface oil into the product and hot steam discharge out from the product coincides (Moreira and Barrufet, 1998; Bouchon *et al.*, 2003; Brannan *et al.*, 2014). As the steam condensation changes proportionally to the reducing temperature of the product along the post -frying process, more surface oil leads into the product, thus increasing the product's calories (Vitrac *et al.*, 2000; Dash *et al.*, 2022). The application of the products with hydrocolloid batter indicated a promising solution, as discussed in the literature. The application minimizes the product surface properties' complexity (Salvador *et al.*, 2008; Tavera-Quiroz *et al.*, 2012; Pahade and Sakhale, 2012; Garmakhany *et al.*, 2014; Angor, 2016) in terms of surface defect, pore size, and roughness by forms a thermo-reversible gel that control the oil and water migration along the frying process (Salehi, 2020). Further investigation by Lua *et al.* (2020) and Lua *et al.* (2022), rigorous mixing of the batter solution prior to the frying process, i.e., ultra-sound processing, enhances the

*Corresponding author.
Email: *mohdnazli@upm.edu.my*

eISSN: 2550-2166
Published by Rynnye Lyan Resources

gel's function as a water absorbance layer that is useful as a barrier for oil uptake of a starchy fried product.

However, to the authors' knowledge, there is no reported work on the modelling work or mechanism to show the interaction of oil and water molecules in the post-frying when the surface temperature was reduced from 180°C (a typical deep-frying condition) to the ambient condition. Thus, the molecular modelling developed in this work was conducted to study the molecular interaction of oil, water, methylcellulose, and potato starch molecules through computational molecular dynamic modelling. The dynamic simulation results in this work are supported by experimental work to verify the modelling results.

2. Materials and methods

2.1 Modelling work and setup

A molecular dynamic simulation was conducted to investigate the oil and water migration through the methylcellulose. The simulation was conducted using MC-coated potatoes versus uncoated ones. The samples were subjected to the typical frying process at 180°C (453K), followed by the post-frying period at 25°C (298K), assuming the substrates were left in the ambient after removal. Biovia Materials Studio software package and Condensed-phase Optimized Molecular Potential for Atomistic Simulation Studies (COMPASS) forcefield were used throughout the simulation work. COMPASS forcefield can accurately predict an extensive range of organic and inorganic molecules (Sun, 1998; Azmi *et al.*, 2020). It was reported that COMPASS forcefield has successfully simulated a system containing cellulose and its derivatives, i.e., methylcellulose (Derecskei and Derecskei-Kovacs, 2006), carboxymethylcellulose (Yang *et al.*, 2019). COMPASS has also been applied to simulate a system containing B-type starch (Miyamoto *et al.*, 2011) and amylose (Yang *et al.*, 2013), a polysaccharide that builds up the starch.

Several steps were taken in the simulation work that involved the construction of all molecules involved and refinement, the construction of cell and refinement, construction of layer cell and refinement, and followed by dynamic simulation at 453K and 298K. In the first step, the three-dimensional structure of water (H_2O), methylcellulose (MC), palmitic acid, and oleic acid was constructed using the sketching tool. For the structure methylcellulose, 20 chain lengths were used in the construction using the polymer builder. Then, these molecules were refined by subjecting them to a geometry optimization task to optimize the structure, apply charges, and minimize the energy. An intelligent algorithm was applied for 2000 maximum iterations with the convergence tolerance of 0.0001 kcal/mol for energy, 0.005 kcal/mol/Å for force, and 0.00005Å displacement. The charges were assigned using COMPASS forcefield, and the Ewald summation method was applied for the electrostatic and van der Waals terms with 0.0001 kcal/mol accuracy and 0.5Å buffer width. Unless stated otherwise, the same setup was used for the geometry optimization task throughout the simulation.

2.2 Material model selection

The computations involve ab initio calculations, quantum mechanics, Monte Carlo, free energy and solvation, molecular dynamics, and many other procedures. The molecules involved in this work are B-type starch, cooking oil (palmitic acid, and oleic acid), water (H_2O) and methylcellulose (MC). B-type starch was chosen for the simulation work (Cleven *et al.*, 1978; Imberty and Perez, 1988; Bertoft and Blennow, 2016). Aside from the B-type polymorph, an A-type polymorph which was usually found in plants i.e. maize, and a C-Type polymorph, usually found in grain legume seeds i.e. peas (Wang *et al.*, 2018) also considered. The properties of the polymorphs, the number of water molecules, the geometry of the unit cell, and the packing density were referred to in previous work (Imberty and Perez, 1988; Wang *et al.*, 2018). Cooking oil comprises a mixture of palmitic acid and oleic acid, with 45% and 40% composition, respectively (Syed, 2016).

The B-type starch was constructed from the crystallographic data from Imberty and Perez (1988), which is the currently accepted structure of B-type starch that is improved from the work of Wu and Sarko (1978). The B-type structure has a hexagonal symmetry lattice with P61 space group and unit cell parameters $a = b =$ 18.5Å, c = 54.0Å. The crystal packing of B-type starch with optimized water, methylcellulose, palmitic acid, and oleic acid is shown in Figure 1. The colours represent the individual atom, i.e., red for oxygen, white for hydrogen, and grey for carbon. The lone oxygen atoms in the

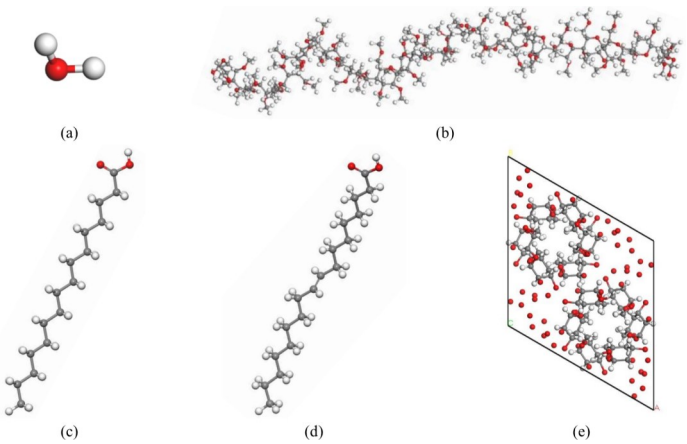

Figure 1. Molecular structure of (a) water, (b) methylcellulose, (c) palmitic acid, (d) olein acid, and (e) B-type starch viewed in the *z*-direction.

https://doi.org/10.26656/fr.2017.9(3).164

crystal packing of B-type starch denote the 36 water molecules between the double helices channels. The hydrogen atom was assigned later in the construction procedure.

Then, an amorphous cell module was used in the second step to build the MC coating cell and oil cell. MC coating cell was constructed using 10 MC and 1000 water molecules with an initial 1 g/cm^3 density. The cell was refined using geometry optimization and dynamic tasks to calculate structure properties, i.e., density and cell parameters in equilibrium. The dynamic simulation was run with one femtosecond (fs) time step for the total simulation time of 500 picoseconds (ps) using an isobaric-isothermal NPT ensemble (constant number of molecules, constant pressure, constant temperature). The total simulation time was limited as the thermo-reversible gel condition occurs between a temperature range of 50°C to 70°C that can be reached in a couple of seconds when subjected to high cooking temperature. Berendsen thermostat and barostat with 0.1ps decay constant were used to control the temperature and pressure at 298K and 1 atm in the post-frying period. Once the successful dynamic simulation was completed, the cell was reconstructed with a 1.020 g/cm^3 density with a dimension of 68 Å × 68 Å × 20.11 Å.

Meanwhile, the oil cell was constructed using 250 palmitic acid and 200 olein acid according to the re-normalized composition based on Syed (2016) with a density of 0.90 g/cm^3 and a dimension of 68 Å × 68 Å × 48.12 Å. The starch cell was constructed by multiplying the length of the B-type starch unit lattice in the *x*, *y,* and *z* direction, and the side edges of the molecules were trimmed to suit a dimension of 68 Å × 68 Å × 32.30 Å. The hydrogen atom was appropriately assigned before the further step was taken.

The third step involved building the B-type starch and MC coating layers using the build layers tool to form the starch/MC cell. Then, the starch/MC cell was refined using a geometry optimization task and dynamic simulation for 100 ps with 1fs timestep using the canonical NVT (constant no of molecules, constant volume, constant temperature) ensemble. The temperature was controlled using a Berendsen thermostat with a 0.1ps decay constant at 298K. In this step, the starch molecules were constrained. As a result, only the MC coating molecules could move freely to form an attachment at the starch surface. After a successful dynamic simulation, the oil layer was added to the cell using the build layers tool to form the starch/MC/oil cell. Since the simulation applied a periodic boundary condition, 30 Å vacuum space was added to the oil layer to avoid oil-starch interaction.

The cell was optimized prior to dynamic simulation in the fourth step. The starch molecules were unconstrained, and dynamic simulation was applied for 100 ps with 0.8 fs time step using the canonical NVT ensemble for the production run. Berendsen thermostat was used to control the temperature at 453K with 0.1ps decay constant. COMPASS forcefield with existing charges was used to calculate the energy using the Ewald summation method for both electrostatic and van der Waals terms with 0.001 kcal/mol accuracy and 0.5Å buffer width. Moreover, the trajectory data was recorded every 1000 steps. After a successful dynamic simulation at 453K, the cell was subjected to dynamic simulation at 298K with the same setup to mimic the cooling process. After that, data analysis and calculation were conducted from the resulting trajectory data. The molecules' transport properties, especially water, were analyzed through the mean square displacement (MSD) data to assess mobility. The MSD of the molecule, concerning its original position, is related to the diffusion coefficient. The diffusion coefficient was calculated from the Einstein relation (Equation 1). Whereby $[r_i(t) - r_i(0)]^2$ is the mean squared displacement of coordinates. While ($r_i(t)$ and $r_i(0)$ stand for the coordinates of nanoparticle *i* at *t* and initial time, respectively (Lara *et al.*, 2012; Shim *et al.*, 2015; Zeng *et al.*, 2018; Azmi *et al.*, 2020).

$$D = \frac{1}{6}\lim_{t\to\infty}\frac{d}{dt}\langle|r_i(t) - r_i(0)|^2\rangle \quad (1)$$

2.3 Experiment work

2.3.1 Methylcellulose properties

A commercial sample of Methylcellulose (MC), (SM4000), was provided by Shinetsu Chemical Co. Ltd., Japan. The methylcellulose has an average degree of substitution, a D.S. value of 1.8, and an average molecular weight of 310 000, determined from light scattering. The MC viscosity range is 4.54 Pa.s at 20°C for a 2 wt% aqueous solution. The aqueous cellulose derivative suspension concentrations of 0.5, 1.0, 1.5, and 2.0 w/v% were subjected to the potato strip prior to the frying process. Each concentration of MC was tested in triplicate.

2.3.2 Experimental preparation of the MC solution

Aqueous methylcellulose solutions were prepared on a wt/vol% according to the hot/cold technique. First, the powder was dispersed into 1/3 of the total water at 80°C and gently mixed with a magnetic stirrer at room temperature until completely dissolved. Subsequently, the beaker was transferred with dispersed MC to a freezer for 12 mins until it reached 10°C. Then 2/3 of water was added, followed by stirring for 30 mins, allowing correct MC hydration. The MC aqueous

https://doi.org/10.26656/fr.2017.9(3).164

solutions were prepared a day before frying and kept at 4°C (Sanz *et al.*, 2004).

2.3.3 Sample preparation

A potato cutter punched the geometry of the potato strip with the dimensions of 8 × 8 × 60 mm. The samples were subjected to a blanching treatment at 85°C for 6 mins, drained, and dried in a convection oven at 150°C for 3 mins to reduce the surface moisture (Pahade and Sakhale, 2012). Then the samples were dipped in the MC hydrocolloid suspensions of 0.5, 1.0, 1.5, and 2.0 w/v% for 10 s (García *et al.*, 2002). A control sample without any coating was also prepared for each batch. Then, the substrates were drained on a metal mesh to remove any excess coating for 3 mins before frying.

2.3.4 Frying condition

Coated and uncoated (control) substrates were fried using an automatic-controlled temperature deep-fat fryer filled with 1.5 L of commercial cooking oil of palm olein. Samples were positioned on a metal mesh basket and fried by immersion in the hot oil at a temperature of 180±2°C for 6 mins (García *et al.*, 2004; Tavera-Quiroz *et al.*, 2012). Used oil was replaced by fresh oil for each batch, and three potato samples were fried/batch.

3. Results and discussion

Figure 2 shows the molecular configuration of uncoated starch in oil at initial (t=0) until reaching the frying temperature at 453K, followed by the post-frying or cooling process at 298K. The molecular configuration was displayed in an in-cell display style, and all the active molecules were coloured for easy observation and comparison. The colour code represents different molecules involved; pink represents palmitic acid; bronze is oleic acid; turquoise is water that was initially embedded in the starch layer. The starch molecules are represented by carbon; grey, oxygen; red, and hydrogen; white. At 0 ps, the system has not undergone dynamic simulation, although it was optimized to reduce the energy to a minimum state. The system consists of the starch (bottom) and the oil layer (upper). None of the molecules was constrained during dynamic simulation. When heated to 453K, the structuring of the particular molecules occurs probably due to the motion and interaction between molecules. Thus, some molecules moved out of their original coordinate. Mass transfer between water and oil occurs in opposite directions within the system. Therefore, the oil layer moves closer to the starch surface during the dynamic simulation. At the end of the dynamic simulation, 100 ps, the molecular structuring was more prominent, and the attachment of oil molecules was noticed on the surface of the starch layer. Slight changes in the central molecular structure of starch represented by the polysaccharide chain were also observed, although they still retain their double helices arrangement. The molecular structure of starch was hard to move around due to its double helices structure, and the torsional changes between the atoms mainly caused the changes. The movement of water molecules in the channel between the double helices structure also caused the starch structure to lose its order as the water moves through the channel once the dynamic starts. The water molecules close to the interface diffused into the oil layer as the dynamic progressed.

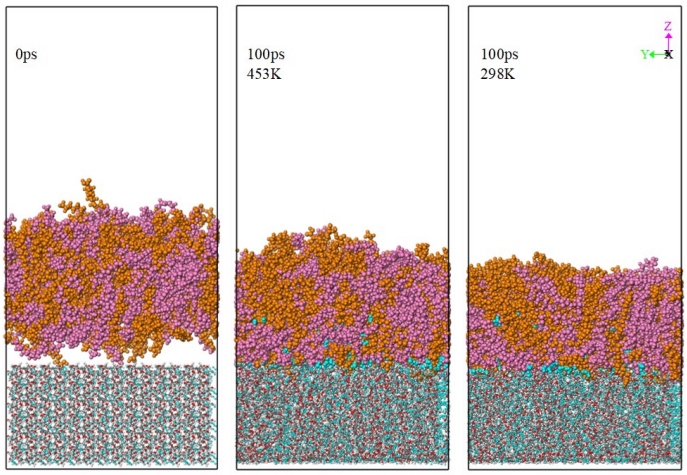

Figure 2. Molecular configuration of uncoated starch reaction with oil during frying (453K) and cooling (298K) at 100 ps. Colour code, palmitic acid; pink, oleic acid; bronze, water; turquoise that initially in the starch layer; Starch atom, carbon; grey, oxygen; red and hydrogen; white.

Water molecules diffused into the oil layer are displayed in CPK style (turquoise colour). At the end of dynamic simulation~ at 100 ps, a large number of water molecules diffuse out from the substrate. After the frying process, the system was assumed to be covered with surface oil and underwent a cooling process at 298K for 100 ps. Starch molecules have contracted at the end of the simulation compared to the system at 453K, at 298K. Further changes in the molecular configuration were also observed due to the different temperature changes. At 298K, it was observed that the oil molecules have further penetrated beneath the starch's surface layer, representing the beginning of the capillary force mechanism to absorb the surface oil into the substrate. Meanwhile, the diffused water molecules in the surface oil layer during the post-frying process were also observed. The activities for water molecules diffuse into the oil layer and oil movement into the starch surface are discussed further in Figure 4.

The molecular dynamics of methylcellulose (MC) coating during the frying and post-frying process were also investigated, as shown in Figure 3. The same display style and colour code were employed with MC in

https://doi.org/10.26656/fr.2017.9(3).164

green, and water was initially in the MC layer in dark blue. Like the uncoated starch frying process, the system in Figure 3 was optimized to reduce energy before the dynamic simulation. The system consists of three layers the starch layer (bottom), the coating layer (middle), and the oil layer (upper). At 0ps, the starch structure retains its ordered arrangement as the dynamic has not begun. During simulation, the heat was applied at 453K, and motions of molecules were observed that led to different molecular structuring as the dynamic progressed. At 100 ps, oil molecules' attachment to the coating layer's surface was observed. The oil molecules penetrated deeper inside the coating layer, and some molecules attached to the starch's surface. At 498 K, it is interesting to note that oil molecules diffuse into the large opening of MC's layer, indicating the beginning of crust and structural oil formation. At 298K, oil absorption into the MC layer was noticed. Interestingly, the oil molecules could not penetrate deeper to reach the substrate layer compared to the uncoated ones. From our hypothesis, it is caused by the MC layer's capability to control the oil uptake mechanism, as portrayed by other workers.

The top-view condition of MC layer voids is also shown at the bottom of Figure 3. Before the dynamic simulation at 0ps, only a small pore was noticed on the z-direction of the methylcellulose coating layer. After 100ps of 453K, the coating layer loses its original shape as the interaction occurs, whereby the pores or channels are formed at the end of the simulation. Re-organization of pores occurs at high temperatures due to the migration of water and oil in opposite directions. This phenomenon is expected as new pores form, while the old pores could be collapsed throughout the heating process. After cooling at 298K, the pores retain their position and coordinate, although there is a slight change in the pore size of the void. It was difficult to determine the exact pore size of methylcellulose as the shape was not uniform. However, the pore diameter ranges were estimated to be between 5 to 20 Å at 453K and 3 to 16 Å at 298K. The pore size of the coated potatoes was smaller than the uncoated ones, as reported by Patsioura *et al*. (2015). The pore size at the post-frying was smaller than in the frying process. The occupied volume of the methylcellulose coating was also determined. The pores contraction volume of frying and post-frying was 78736.44 $Å^3$ and 76508.51 $Å^3$, respectively. The frying process also causes surface rupture due to increased internal pressure. In contrast, the cooling process causes the layer to collapse when water evaporation is reduced and eventually stopped due to the reduced internal capillary pressure. The same phenomenon was also observed in the earlier work, reducing the pore size and volume (Ziaiifar *et al.*, 2010)

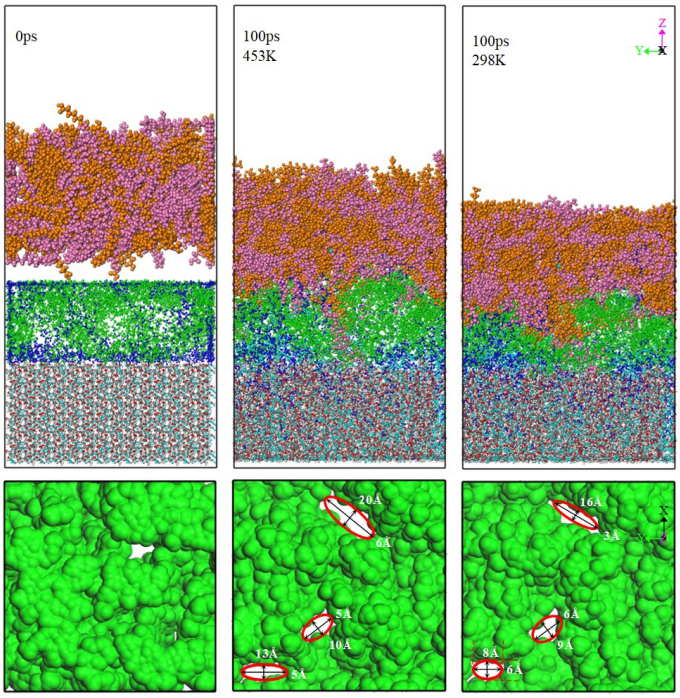

Figure 3. Molecular configuration of methylcellulose (MC)-coated starch reaction with heated palm oil during frying (453K) and followed by the post-frying (298K) at 100ps. Below is the molecular configuration indicating methylcellulose pore formation from the top view at the respective temperature. Colour code, palmitic acid; pink, oleic acid; bronze, water; turquoise that initially in the starch layer, starch atom, carbon; grey, oxygen; red and hydrogen; white, green, methylcellulose; dark blue, water originally in methylcellulose layer; grey.

Figure 4a and Figure 4b show the mean square displacement (MSD) of specific molecules in uncoated and MC-coated potatoes, respectively, at different temperatures. The MSD was analyzed from the trajectory data after a successful dynamic simulation. It is noted that the analyzed water molecules found in the oil region originally came from starch. Simultaneously, all oil molecules were also considered for MSD analysis. The MSD value of water and oil increases with time, as indicated in Figure 4. The slope of the MSD curve is proportional to the diffusivity of molecules, whereby the displacement of molecules is associated with their movement. The diffusion coefficient was calculated from the slope of the MSD curve and Equation 1 and the data was tabulated in Table 1. The diffusion coefficient of molecules corresponds to the MSD curve whereby the diffusion coefficient of water and oil at 453K is higher than that of water and oil at 298K for both uncoated and MC-coated substrates. During the frying process, the MSD value of water in oil of MC-coated substrate showed a greater value at 453K, but it indicated a lower oil MSD value compared to the uncoated one with a diffusion coefficient value of 1.0760 versus 0.6345 (10^{-4} cm^2/s) and 0.1375 versus 0.3513 (10^{-4} cm^2/s). This indicates that the MC layer promotes the water

https://doi.org/10.26656/fr.2017.9(3).164

Table 1. Transport properties of water and oil in uncoated and coated starch at 453K and 298K.

System	Uncoated starch		Coated starch	
Temperature (K)	453K	298K	453K	298K
Diffusion coefficient of water in oil (10^{-4} cm^2/s)	0.6345	0.0796	1.0760	0.9353
Diffusion coefficient of oil into starch (10^{-4} cm^2/s)	0.3513	0.0731	0.1375	0.1334

molecules migration during frying out from the substrate but limits the oil penetration into starch. In the post-frying period (298K), the MSD value of water in oil of MC-coated substrate still showed a greater value than the uncoated one with a diffusion coefficient of 0.9353 versus 0.0796 (10^{-4} cm^2/s). Surprisingly greater oil MSD value was also noticed in the MC-coated substrate than in the uncoated one, with a diffusion coefficient value of 0.1334 and 0.0731 (10^{-4} cm^2/s), respectively.

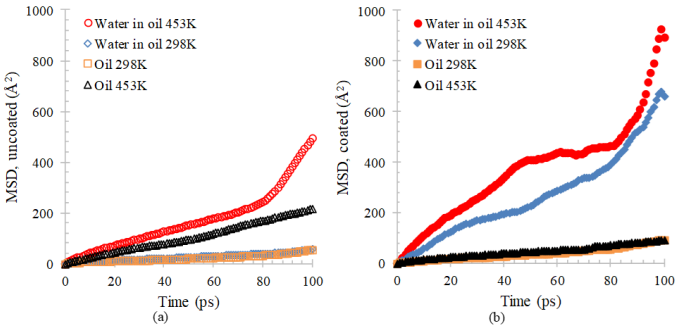

Figure 4. Mean square displacement (MSD) of different water molecules moves to oil (water in oil) and oil molecules move into starch (oil) of (a) uncoated and (b) MC-coated substrate at frying temperature, 453K, and post-frying, 298K.

In the post-frying period, the low diffusion coefficient values of coated and uncoated ones simultaneously allowed the oil molecules to diffuse into the substrate through the interfacial layer of both conditions. In the case of the uncoated substrate, the diffused oil penetrates deeper into the substrate region. In the case of coated ones, the oil molecules probably spread onto the substrate's outer layer as the surface roughness of MC coated increases due to crust formation at frying temperature. A similar observation was reported by Lara *et al.* (2012). They noticed that the diffusion coefficient of investigated silica nanoparticles in brine solution was higher at 350 K than at 300 K.

Figure 4 also shows that the MSD for water is always higher than oil at any respective temperatures, indicating that water molecules possess high mobility and, therefore, it is easier for water molecules to be diffused in the system. It is expected for smaller molecules to have a higher diffusion compared to larger molecules. Water molecules are much smaller than oil, so the mobility and diffusion coefficient are also higher.

The mechanisms of oil uptake during cooling remain only partly understood. However, many workers agree that oil uptake occurs during the cooling period and depends on the amount of surface oil attached to the substrate surface. To summarise the Figure 4 and Table 1 output, the MC layer provides a protective barrier that reduces the oil uptake and serves as a gate by allowing large numbers of water molecules from starch into the oil layer and small numbers of oil into the starch region based on the pore size opening at the outmost layer. The evidence can be noticed from the consistent diffusion coefficient of water in oil during frying and cooling, with 1.0760×10^{-4} cm^2/s and 0.9353×10^{-4} cm^2/s, respectively. A similar trend was also found diffusion coefficient of oil in the starch layer, with 0.1375×10^{-4} cm^2/s and 0.1334×10^{-4} cm^2/s, respectively.

The case was different in uncoated starch, whereby a significant difference was noticed between the diffusion coefficient of water in oil and the diffusion coefficient of oil in the starch layer for both conditions. As a result, two different molecules' movements can be noticed during frying and cooling, probably due to the pore opening difference at the outmost layer of the fried substrate. For example, low numbers of water molecules were found migrating from starch to the oil layer, resulting in a low number of oil penetrating into starch during cooling as in Figure 4(a), compared to coated ones in Figure 4(b), which can explain further with the experimental results.

Experimental work was done by subjecting a potato strip to several MC batter concentrations of 0.5 w/v% to 2 w/v% prior to the frying process to support the modelling work. Figure 5 shows the comparison data of water loss and oil uptake when the sample concentration was varied. From Figure 5, it was noticed that the MC layer had limited the oil and water migration of the substrate at any MC concentrations (wt/vol%). The highest water loss was noticed in the control group, as predicted earlier from the modelling results. About 81.2% water loss and 46.2% oil uptake were noticed from the uncoated substrate, while the average of all MC -coated substrates was between 78.5% and 28%, respectively. The results agreed with the simulation work as the consistent diffusion coefficient of water in oil during and oil into starch of frying and post-frying process except for the case of the uncoated substrate, in Figure 4(a) and Table 1. Greater oil uptake was noticed for uncoated samples as the diffusion coefficient of water in oil and oil into starch were insignificant, which was 0.63 and 0.35 ($\times10^{-4}$ cm^2/s) during frying and 0.08 and 0.07 ($\times10^{-4}$ cm^2/s), in the cooling system. Thick crust formation was thicker in uncoated samples; hence, a large amount of surface oil trapped in the crust's pore

https://doi.org/10.26656/fr.2017.9(3).164

influenced the diffusion coefficient value of water in oil and oil into starch, which was unnoticed in the simulation work. Even though the MC concentration varied from 0.5-2 wt/vol%, the water and oil relationship remained, as indicated in Figure 5. Therefore, thicker crust formation probably contributes to the structural oil, contributing to a large amount of oil consumption when consumed.

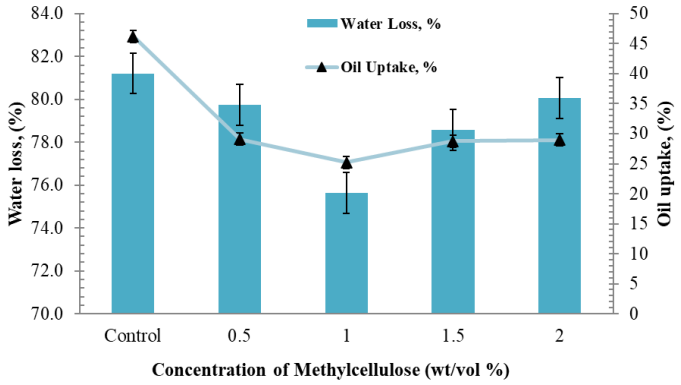

Figure 5. Relative variation of water loss, (%) of fried potato strips coated at different MC concentrations (wt/vol%). Control was prepared without any batter coating. All sample was fried at 180°C for 6 mins.

Morphology analysis of the substrate's surface was conducted using a microscope in Figure 6, and the obtained images were subjected to the image J analysis. Table 2 summarizes surface analysis characteristics, including the pore numbers, average pore size, and total pore area. The 1.0 wt/vol% of MC concentration shows the lowest number of pores and smallest total pores area of all samples, which probably contributes to the lowest water loss and oil uptake, which was noticed in Figure 5. The pore size and total pores area were assumed to act like gates that allow the water migration, which was also correlated with the consistent diffusion coefficient value of water in oil and oil into starch as described earlier. A greater water flux rate into the oil region is also expected for narrow entrance, which was noticed in all MC-coated samples compared to the uncoated ones. Therefore, the lower oil uptake was noticed for all MC-coated samples compared to the uncoated ones.

Table 2. Number of pores and pore average area of methylcellulose, MC coated and non-coated fried potato strips.

MC batter concentration, w/v%	Pores number	Average pore size (mm)	Total pores area (mm^2)
Control	867	48.96	25107
0.5	618	40.25	24865
1.0	526	45.93	24157
1.5	573	42.89	24558
2.0	632	39.15	24730

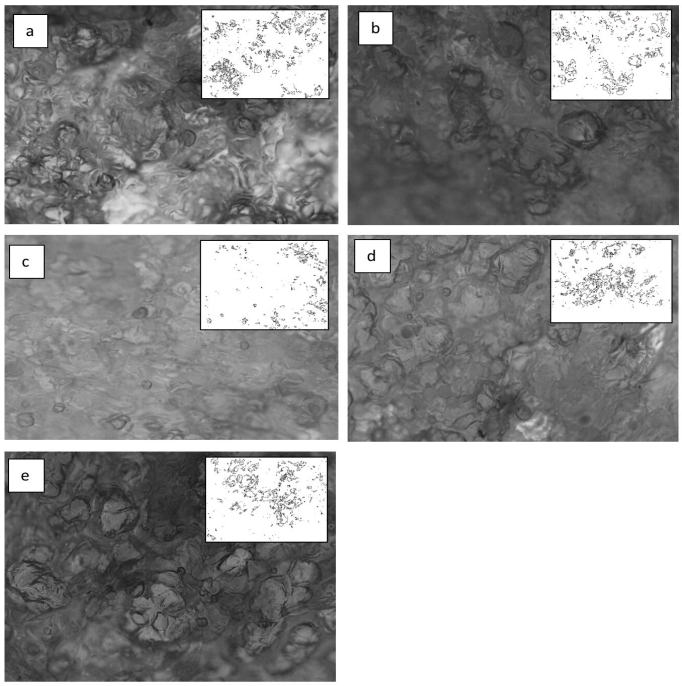

Figure 6. Light microscope photograph analysis of the surface morphology of uncoated and MC-coated fried potato strips. (a) uncoated (control), (b) 0.5 wt/vol% MC coated, (c) 1.0 wt/vol% MC coated, (d) 1.5 wt/vol% MC coated, and (e) 2.0 wt/vol% MC coated. Image J analysis of the analyzed area (grey colour) was shown on the top right of the picture.

4. Conclusion

The methylcellulose (MC) layer provides a barrier to reduce the oil uptake by providing consistent water molecules' migration from the substrate into the oil region, preventing oil penetration into starch. The modelling work explains the phenomenon that limits the oil molecules from diffusing at the interfacial layer compared with the uncoated one. In the case of the uncoated ones, the oil uptake was not from the oil penetration into starch but from the structural oil trapped inside the crust. The modelling work could not describe the phenomenon, but it was eventually verified via the experimental work.

Conflict of interest

All authors declare no conflict of interest.

Acknowledgements

This work was supported by the Fundamental Research Grant Scheme, FRGS/1/2019/TK02/UPM/02/11 (554098), Ministry of Higher Education (MOHE) Malaysia. The work facilities were provided by the Faculty of Engineering, Universiti Putra Malaysia, Serdang, Malaysia, Universiti Teknologi MARA, Shah Alam, Malaysia and Universiti Malaysia Pahang, Pahang, Malaysia.

https://doi.org/10.26656/fr.2017.9(3).164

References

Angor, M.M. (2016). Reducing Fat Content of Fried Potato Pellet Chips Using Carboxymethyl Cellulose and Soy Protein Isolate Solutions as Coating Films. *Journal of Agricultural Science*, 8(3), 162. https://doi.org/10.5539/jas.v8n3p162

Azmi, N.S.M., Abu Bakar, N.F., Tengku Mohd, T.A. and Azizi, A. (2020). Molecular dynamics simulation on CO_2 foam system with addition of SiO_2 nanoparticles at various sodium dodecyl sulfate (SDS) concentrations and elevated temperatures for enhanced oil recovery (EOR) application. *Computational Materials Science*, 184, 109937. https://doi.org/10.1016/j.commatsci.2020.109937

Bertoft, E. and Blennow, A. (2016). Structure of Potato Starch. In Singh, J. and Kaur, L. (Eds.) Advances in Potato Chemistry and Technology. 2nd ed. USA: Academic Press. https://doi.org/10.1016/B978-0-12-800002-1.00003-0

Bouchon, P., Aguilera, J.M. and Pyle, D.L. (2003). Structure Oil-Absorption Relationships during Deep-Fat Frying. *Journal of Food Science*, 68(9), 2711–2716. https://doi.org/10.1111/j.1365-2621.2003.tb05793.x

Brannan, R.G., Mah, E., Schott, M., Yuan, S., Casher, K.L., Myers, A. and Herrick, C. (2014). Influence of ingredients that reduce oil absorption during immersion frying of battered and breaded foods. *European Journal of Lipid Science and Technology*, 116(3), 240-254. https://doi.org/10.1002/ejlt.201200308

Cleven, R., van Den Berg, C. and van der Plas, L. (1978). Crystal Structure of Hydrated Potato Starch. *Starch - Stärke*, 30(7), 223-228. https://doi.org/10.1002/star.19780300703

Dash, K.K., Sharma, M. and Tiwari, A. (2022). Heat and mass transfer modeling and quality changes during deep fat frying: A comprehensive review. *Journal of Food Process Engineering*, 45(4), e13999. https://doi.org/10.1111/jfpe.13999

Derecskei, B. and Derecskei-Kovacs, A. (2006). Molecular dynamic studies of the compatibility of some cellulose derivatives with selected ionic liquids. *Molecular Simulation*, 32(2), 109–115. https://doi.org/10.1080/08927020600669627

García, M.A., Ferrero, C., Campana, A., Bértola, N., Martino, M. and Zaritzky, N. (2002). Edible coatings from cellulose derivatives to reduce oil uptake in fried products. *Food Science and Technology International*, 10(5), 339–346. https://doi.org/10.1177/1082013204047564

García, M.A., Ferrero, C., Campana, A., Bértola, N., Martino, M. and Zaritzky, N. (2004). Methylcellulose coatings applied to reduce oil uptake in fried products. *Food Science and Technology International*, 10(5), 339–346. https://doi.org/10.1177/1082013204047564

Garmakhany, A.D., Mirzaei, H.O., Maghsudlo, Y., Kashaninejad, M. and Jafari, S.M. (2014). Production of low fat french-fries with single and multi-layer hydrocolloid coatings. *Journal of Food Science and Technology*, 51(7), 1334–1341. https://doi.org/10.1007/s13197-012-0660-9

Imberty, A. and Perez, S. (1988). A revisit to the three-dimensional structure of B-type starch. *Biopolymers*, 27(8), 1205-1221. https://doi.org/10.1002/bip.360270803

Lara, L.S. de, Michelon, M.F. and Miranda, C.R. (2012). Molecular dynamics studies of fluid/oil interfaces for improved oil recovery processes. *Journal of Physical Chemistry B*, 116(50), 14667-14676. https://doi.org/10.1021/jp310172j

Lua, H.Y., Naim, M.N., Mohammed, M.A.P., Hamidon, F. and Abu Bakar, N.F. (2020). Effects of ultrasonicated methylcellulose coating on French fries during deep frying process. *Journal of Food Process Engineering*, 43(2), e13332. https://doi.org/10.1111/jfpe.13332

Lua, H.Y., Naim, M.N., Mohammed, M. A.P., Hamidon, F., Abu Bakar, N.F., Vangnai, K., Jittanit, W. and Teh, H.F. (2022). Inhibition of acrylamide formation in potato strip by ultrasonic-treated methylcellulose batter. *International Journal of Food Science and Technology*, 57(6), 3292-3302. https://doi.org/10.1111/ijfs.15652

Miyamoto, H., Ago, M., Yamane, C., Seguchi, M., Ueda, K. and Okajima, K. (2011). Supermolecular structure of cellulose/amylose blends prepared from aqueous NaOH solutions and effects of amylose on structural formation of cellulose from its solution. *Carbohydrate Research*, 346(6), 807-814. https://doi.org/10.1016/j.carres.2011.01.037

Moreira, R.G. and Barrufet, M.A. (1998). A New Approach to Describe Oil Absorption in Fried Foods: A Simulation Study. *Journal of Food Engineering*, 35(1), 1-22. https://doi.org/10.1016/S0260-8774(98)00020-X

Pahade, P.K. and Sakhale, B.K. (2012). Effect of blanching and coating with hydrocolloids on reduction of oil uptake in french fries. *International Food Research Journal*, 19(2), 697-699.

Salehi, F. (2020). Effect of coatings made by new hydrocolloids on the oil uptake during deep-fat frying: A review. *Journal of Food Processing and*

Preservation, 44(11), e14879. https://doi.org/10.1111/jfpp.14879

Salvador, A., Sanz, T. and Fiszman, S.M. (2008). Performance of methyl cellulose in coating batters for fried products. *Food Hydrocolloids*, 22(6), 1062-1067. https://doi.org/10.1016/j.foodhyd.2007.05.015

Sanz, T., Salvador, A. and Fiszman, S.M. (2004). Effect of concentration and temperature on properties of methylcellulose-added batters Application to battered, fried seafood. *Food Hydrocolloids*, 18(1), 127-131. https://doi.org/10.1016/S0268-005X(03)00050-X

Shim, H.M., Kim, H.S. and Koo, K.K. (2015). Molecular modeling on supersaturation-dependent growth habit of 1,1-diamino-2,2-dinitroethylene. *Crystal Growth and Design*, 15(4), 1833-1842. https://doi.org/10.1021/cg5018714

Sun, H. (1998). Compass: An ab initio force-field optimized for condensed-phase applications - Overview with details on alkane and benzene compounds. *Journal of Physical Chemistry B*, 102 (38), 7338-7364. https://doi.org/10.1021/jp980939v

Syed, A. (2016). Chapter 4 - Oxidative Stability and Shelf Life of Vegetable Oils. In Hu, M. and Jacobsen, C. (Eds.) Oxidative Stability and Shelf Life of Foods Containing Oils and Fats. USA: Academic Press and AOCS Press. https://doi.org/10.1016/B978-1-63067-056-6.00004-5

Tavera-Quiroz, M.J., Urriza, M., Pinotti, A. and Bertola, N. (2012). Plasticized methylcellulose coating for reducing oil uptake in potato chips. *Journal of the Science of Food and Agriculture*, 92(7), 1346-1353. https://doi.org/10.1002/jsfa.4704

Vitrac, O., Trystram, G. and Raoult-Wack, A.L. (2000). Deep-fat frying of food: Heat and mass transfer, transformations and reactions inside the frying material. *European Journal of Lipid Science and Technology*, 102(8-9), 529-538. https://doi.org/10.1002/1438-9312(200009)102:8/9<529::aid-ejlt529>3.0.co;2-f

Wang, T.L., Bogracheva, T. Y. and Hedley, C.L. (2018). As simple as A, B, non-A, non-B. *The Lancet Gastroenterology and Hepatology*, 3(2), 82. https://doi.org/10.1016/S2468-1253(17)30405-3

Wu, H.-C.H. and Sarko, A. (1978). The double-helical molecular structure of crystalline a-amylose. *Carbohydrate Research*, 61(1), 27-40. https://doi.org/10.1016/S0008-6215(00)84464-X

Yang, L., Zhang, B., Yi, J., Liang, J., Liu, Y. and Zhang, L. M. (2013). Preparation, characterization, and properties of amylose-ibuprofen inclusion complexes. *Starch/Staerke*, 65(7-8), 593-602. https://doi.org/10.1002/star.201200161

Yang, S., Huang, Y., Su, S., Han, G. and Liu, J. (2019). Hybrid humics/sodium carboxymethyl cellulose water-soluble binder for enhancing the electrochemical performance of a Li-ion battery cathode. *Powder Technology*, 351, 203-211. https://doi.org/10.1016/j.powtec.2019.04.027

Zeng, Y., Li, K., Zhu, Q., Wang, J., Cao, Y. and Lu, S. (2018). Capture of CO_2 in carbon nanotube bundles supported with room-temperature ionic liquids: A molecular simulation study. *Chemical Engineering Science*, 192, 94-102. https://doi.org/10.1016/j.ces.2018.07.025

Ziaiifar, A. M., Courtois, F. and Trystram, G. (2010). Porosity development and its effect on oil uptake during frying process. *Journal of Food Process Engineering*, 33(2), 191-212. https://doi.org/10.1111/j.1745-4530.2008.00267.x

